Journal of Molecular Graphics and Modelling 29 (2010) 148–156

Contents lists available at ScienceDirect

Journal of Molecular Graphics and Modelling

journal homepage: www.elsevier.com/locate/JMGM

Structural and mechanistic insights into a novel non-competitive Kunitz trypsin inhibitor from *Adenanthera pavonina* L. seeds with double activity toward serine- and cysteine-proteinases

Ludovico Migliolo[a,b], Adeliana S. de Oliveira[a], Elizeu A. Santos[a], Octavio L. Franco[b,c,*], Maurício P. de Sales[a]

[a] *Laboratório de Química e Função de Proteínas Bioativas, Departamento de Bioquímica, Centro de Biociências, Universidade Federal do Rio Grande do Norte, Natal, RN, Brazil*
[b] *Centro de Análises Proteômicas e Bioquímicas, Programa de Pós-Graduação em Ciências Genômicas e Biotecnologia, Universidade Católica de Brasília, Brasília, Brazil*
[c] *Departamento de Biologia, Universidade, Federal de Juiz-de-Fora, Minas Gerais, Brazil*

ARTICLE INFO

Article history:
Received 17 February 2010
Received in revised form 11 May 2010
Accepted 14 May 2010
Available online 25 May 2010

Keywords:
Adenanthera pavonina
Non-competitive proteinase inhibitor
Kunitz family
Binding sites
Homology modeling
Docking studies

ABSTRACT

Kunitz proteinase inhibitors are widely distributed in legume seeds, and some of them have the ability to inhibit two different classes of enzymes. In this report, novel insights into three-dimensional structure and action mechanism of ApKTI, an *Adenanthera pavonina* Kunitz trypsin inhibitor, were provided to shed some light on an unconventional non-competitive activity against trypsin and papain. Firstly, ApKTI was purified by two tandem-size molecular exclusion chromatography high resolutions, Sephacryl S-100 and Superose 12 10/300 GL. Purified ApTKI showed molecular mass of 22 kDa and higher affinity against trypsin in comparison to papain, while the bifunctional inhibitor presented lower inhibitory activity. Moreover, *in vitro* assays showed that ApKTI has two independent interaction sites, permitting simultaneous inhibition to both enzymes. Theoretical three-dimensional structures of ApTKI complexed to both target proteinases were constructed in order to determine interaction mode by using Modeller v9.6. Since the structure of no non-competitive Kunitz inhibitor has been elucidated, ApTKI-trypsin and ApTKI-papain docking were carried out using Hex v5.1. *In silico* experiments showed that the opposite inhibitor loop interacts with adjacent sites of trypsin (Arg^{64}, Ser^{107}, Arg^{88} and Lys^{108}) and papain (Gln^{51}, Asp^{172} and Arg^{173}), probably forming a ternary complex. Unusual residue substitutions at the proposed interface can explain the relative rarity of twin trypsin/papain inhibition. The predicted non-coincidence of trypsin and papain binding sites is completely different from that of previously proposed inhibitors, adding more information about mechanisms of non-competitive plant proteinase inhibitors.

1. Introduction

Kunitz-type proteinaceous inhibitors reversibly interact with enzyme targets, forming stable complexes influencing their catalytic activities in competitive and non-competitive ways [1–3]. These inhibitors have been widely isolated and characterized from plants [2–8], normally occurring as single polypeptide chains [9–11]. Nevertheless, inhibitors from the Mimosoideae subfamily have shown an unusual dimeric conformation sustained by disulphide bridges. These bioactive macromolecules have been implicated in various physiological functions, such as regulation of proteolytic cascades and safe storage of proteins, as well as defense molecules against plant pests and pathogens [12]. Kunitz-type inhibitors are characterized by molecular masses around 20 kDa, a low cysteine content forming two disulphide bonds and a common structural fold composed of a β-trefoil formed by 12 antiparallel β-strands with long interconnecting loops presenting one or two reactive sites for serine proteinases [11,13–16]. Although several common properties have been found in Kunitz inhibitors, some secondary activities have been reported in the literature. Previous studies showed that the Kunitz trypsin inhibitor of *Prosopis juliflora* (PjTKI) possesses a competitive inhibition mechanism directly interacting between the P1 inhibitor site (Arg^{64}) and the S1 site in target trypsin (Ser^{195}). Moreover, PjTKI also showed an unexpected inhibitory activity against papain, a cysteine-proteinase present in the digestive system of several phytophagous insect-pests [6]. The *in silico* structural model of PjTKI demonstrated that interaction sites for trypsin and papain overlap [17]. This bifunctional property was detected in several Kunitz-type inhibitors, such as

Abbreviations: ApTKI, *Adenanthera pavonina* trypsin Kunitz inhibitor; FPLC, fast protein liquid chromatography; PjTKI, *Prosopis juliflora* trypsin Kunitz inhibitor; SKTI, soybean Kunitz trypsin inhibitor; TCA, trichloroacetic acid.

* Corresponding author at: SGAN Quadra 916, Av. W5 Norte, Módulo C 70.790-160 Brasília, DF, Brazil. Tel.: +55 61 3448 7167; fax: +55 61 3347 4797.
E-mail addresses: ocfranco@gmail.com, ocfranco@pos.ucb.br (O.L. Franco).

1093-3263/$ – see front matter © 2010 Elsevier Inc. All rights reserved.
doi:10.1016/j.jmgm.2010.05.006

proteins isolated from seeds of *Acacia confusa*, *Caesalpinia bonbuc* (L.), *Enterolobium contortisiliquum*, *Erythrina variegata*, *Swartizia pickelli* (inhibitory activities toward trypsin and chymotrypsin), *Pithecellobium dumosum*, *Crotalaria pallida* (inhibitory activities toward trypsin, chymotrypsin and papain), *Delonix regia* (inhibitory activities toward trypsin and human plasma kallikrein), *P. juliflora* (inhibitory activity toward papain and trypsin) [3,6,7,18–24]. In summary, the present study aims to provide new biochemical information about an unusual non-competitive Kunitz inhibitor with the ability to inhibit two different proteolytic enzyme classes, shedding some light on mechanistic inhibitory strategies. For these, a combination of *in vitro* and *in silico* experiments were conducted providing evidence that ApTKI binding sites for trypsin and papain do not overlap, as previously described in the literature for other inhibitors. Since potential predators whose cysteine-proteinase activity was inhibited might be unable to bypass that inhibition through the expression of serine proteinases and vice-versa, the inhibitor here described could be a highly attractive candidate for development into an inhibitor to be expressed by transgenic crops.

2. Material and methods

2.1. Material

Reagents utilized were porcine pancreatic trypsin, papain and azocasein acquired from Sigma Co. (USA) and trichloroacetic acid (TCA), and protein molecular weight markers were purchased from Fermentas Life Science. *Adenanthera pavonina* seeds were obtained from the seed bank from IBAMA (Brazilian Environmental Institute of natural and renewable resources) in Natal, RN, Brazil.

2.2. In vitro inhibitor and enzyme interactions

2.2.1. ApTKI purification

Crude protein extract was obtained from 100 g of dry seeds by continuous stirring with 50 mM sodium tetraborate buffer, pH 7.5 (1:10, w/v), at room temperature for about 3 h. After centrifugation for 30 min at 12,000 × *g* at 4 °C, precipitate was discarded and supernatant was isolated from crude seed extract in a range of 40–60% of ammonium sulfate. After dialyses, the rich fraction was applied to a size exclusion chromatography (S-100 high resolution Sephacryl) equilibrated with Tris–HCl 50 mM, pH 7.5. Protein fractions were dialyzed against distilled water, lyophilized and further stored at −20 °C. The fraction that showed inhibitory activity was applied onto a FPLC Superose 12 10/300 GL chromatography at a flow rate of 0.5 mL min^{-1} detected at absorbance of 280 nm. Resin was previously equilibrated with Tris–HCl 50 mM, pH 7.5 buffer. The purified fraction, known as ApTKI, was dialyzed against distilled and lyophilized water for subsequent assays.

2.2.2. Enzyme and enzyme inhibitory assays

Proteolytic inhibitory activities were conducted by using 1% azocasein solution as substrate according to Langner et al. [25]. Stoichiometric proportions between inhibitor and enzyme activities were obtained by construction of a dose response curve, and these values were used in the binary complex assays. Binary ApTKI–papain and ApTKI–trypsin complexes were evaluated against porcine trypsin and papaya latex papain. The assays were performed in 50 mM Tris–HCl pH 7.5 buffer. The reaction for porcine trypsin was started with 120 μL solution of 25 mM HCl, and after 30 min the reaction was stopped with TCA 20% final concentration after hydrolysis 200 μL of azocasein at 1%. The binary papain–inhibitor complex was added to the trypsin reaction, with the aim of observing the inhibitory activity. Papain reaction was started with 40 μL of solution containing L-cysteine 50 mM and EDTA 0.02 M, pH 8.0; after 30 min the reaction was stopped with TCA 20% final concentration, after carrying out hydrolysis on 200 μL of substrate at 1%. The binary trypsin–inhibitor complex was added to the papain reaction, with the aim of observing the inhibitory activity. Both reactions were centrifuged at 12,000 × *g* for 10 min at room temperature, and 500 μL supernatant was alkalinized by adding 500 μL of NaOH at 2 N. The absorbance was measured at 440 nm. The blank tests without presence of the substrate were analyzed and added after 30 min, when the reaction was stopped with TCA 20% final concentration. All assays were conducted in triplicate.

2.3. In silico inhibitor and enzyme interactions

2.3.1. Molecular modeling

Primary sequences of ApTKI were obtained from NCBI gene bank with accession numbers of α (gi: 124152) and β chains (gi: 124153) [26]. PSI-BLAST [27] was used for template data mining. Soybean Kunitz inhibitor PDB: 1avw [13], which shows 38% identity, was chosen as template. An ApTKI three-dimensional model was constructed by using crystal atomic coordinates of free SKTI at a resolution of 1.9 Å. No complexed structure was utilized, since ApTKI inhibited trypsin by a non-competitive mechanism (data reported here). Five models were constructed by using Modeller v9.6 [28] where protein tertiary structure models were chosen for their fulfillment of spatial restraints, taking into account loops energy minimization conducted by default parameters [29]. Predicted ApTKI model evaluation, i.e., geometry, stereochemistry, and energy distributions in the models, was performed using PROSA II to analyze packing and solvent exposure characteristics and PROCHECK for additional analysis of stereochemical quality [30,31]. In addition, RMSD was calculated by overlap of Cα traces and backbones onto the template crystal structure through the program 3DSS [32]. The protein structures were visualized and analyzed on SPDB viewer v.3.7 [33] and Delano Scientific's PYMOL http://pymol.sourceforge.net/.

2.3.2. Molecular docking

HEX v.5.1 [34] program was used to examine possible modes of interaction of ApTKI with papain (9pap), a sulphydryl protease from the latex of the papaya fruit, and trypsin (1fn6) a hydrolase from the porcine pancreas [35,36]. Briefly, this procedure performed global rotational and translational space scan by using Fourier transformations, which rank the output according to surface complementarity and electrostatic characteristics. A list of 500 complexes of papain–inhibitor and trypsin–inhibitor was ranked and biochemical data were available to filter out possible solutions. Previous knowledge of papain and trypsin catalytic site location was used to filter binding models; enzyme–inhibitor complexes were discarded if they showed inhibitor atoms interacting with both catalytic triad papain and trypsin, according to the non-competitive mechanism proposed. Furthermore, the best 50 post-progressing energy minimization model complexes were analyzed by Protein–Protein Interaction Server (http://www.bioinformatics.sussex.ac.uk/protorp/).

3. Results

3.1. Isolation and in vitro models of interaction of ApTKI with trypsin and papain

Bifunctional inhibitor named ApTKI was firstly purified according to Macedo et al. [7] with minor modifications. The soluble protein fraction 40–60 obtained from ammonium sulfate precipitation showed inhibitory activity against trypsin and papain (data not shown). This fraction was applied onto a Sephacryl S-100 column

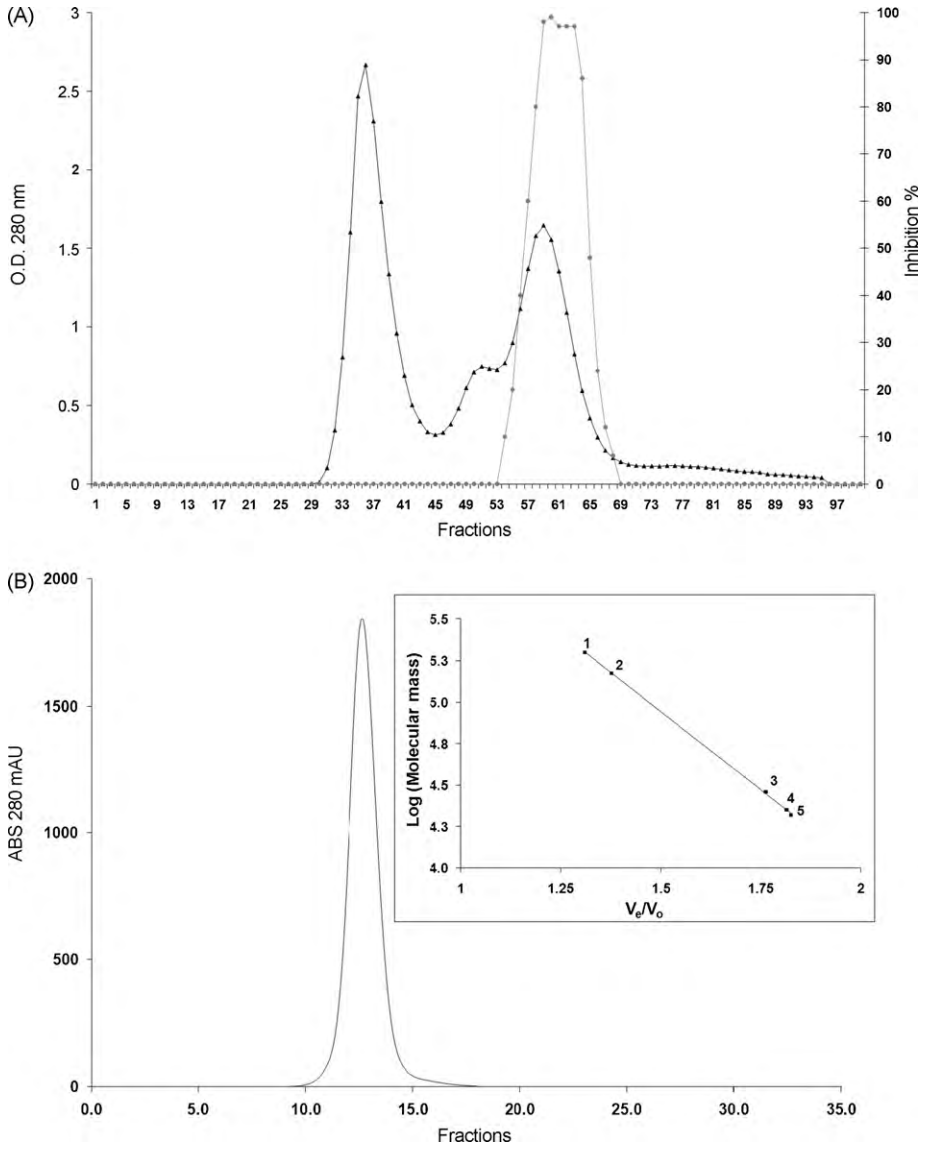

Fig. 1. (A) Chromatography profile (▲) of the soluble protein fraction 40–60 precipitated with ammonium sulfate applied on high resolution Sephacryl S-100 and (●) anti-tryptic activity. (B) Chromatography profile of ApTKI applied on Superose 12 10/300 GL equilibrated buffer Tris–HCl 50 mM, pH 7.5. Protein fraction was collected in flow rate 0.5 mL min^{-1}. Top right square shows molecular masses obtained by calibration curve, (1) β-amylase (200 kDa), (2) alcohol desidrogenase (150 kDa), (3) anhydrase carbonic (29 kDa) and (4) ApTKI (22 kDa), (5) and soybean Kunitz trypsin inhibitor (21 kDa).

previously calibrated with commercial soybean inhibitor (Sigma) yielding three major fractions. The third peak obtained showed highest anti-tryptic activity (Fig. 1A). The anti-tryptic peak was further submitted to a high Superpose 12 10/300 GL chromatography (FPLC), and chromatogram profile (Fig. 1B) showed a single protein fraction with strong inhibitory activity against trypsin and papain (data not shown), now named ApTKI (*A. pavonina* trypsin Kunitz inhibitor). ApTKI was utilized for the establishment of the *in vitro* interaction for trypsin and papain, which were used as interactions models. High purity of seeds was evaluated by SDS-PAGE (data not shown) and molecular mass calibration (Fig. 1B, top square), indicating that ApTKI had a molecular mass of 22 kDa. Equimolar relations of ApTKI to porcine trypsin and papain were also determined. The ApTKI presented an equimolar ratio of 1.97×10^{-10} mM for trypsin (Fig. 2, line A). Moreover, when ApTKI was evaluated against papain an equimolar relation of 5.91×10^{-9} mM was found (Fig. 2, line B). These values were used in the *in vitro* ApTKI–trypsin and ApTKI–papain interactions.

3.2. *In vitro ApTKI–trypsin and ApTKI–papain interactions*

In order to analyze the possibility of ApTKI forming ternary complexes with different interaction loops or to conclude that ApTKI overlaps active sites, as previously observed in PjTKI inhibitor [17], the inhibitor was pre-incubated with trypsin at 37 °C for 15 min under previously described assay conditions and challenged against papain and vice-versa. Purified ApTKI reduced trypsin activity by 97%, exhibiting high affinity for this enzyme class. However when binary complex ApTKI-Papain was assayed for trypsin activity, an interesting reduction of 91% of inhibitory activity was observed. Otherwise, whereas inhibitory activity on papain showed a lower inhibition of 48%, this ability was also observed in the binary complex ApTKI–trypsin, which presented 46%. This last value is similar to the inhibition assay obtained with free inhibitor. Results here provided indicate that the sites of interaction for trypsin and papain were not overlapping, since binary complexes ApTKI–trypsin and ApTKI–papain did not lose their inhibitory activ-

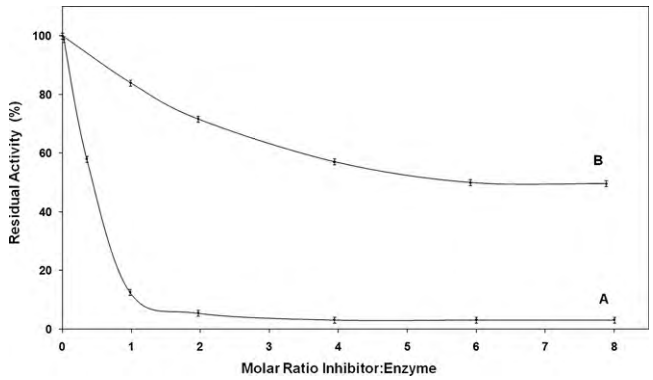

Fig. 2. ApKTI titration curve. (A) Effect of *in vitro* inhibitory activity of ApTKI on serine- (trypsin) and (B) cysteine-proteinase (papain) at pH 7.5.

ities, showing a similar inhibition value to that obtained when the free inhibitor was incubated with both enzymes (Table 1).

3.3. *In silico modeling of ApTKI bound to trypsin and papain*

Considering the limited sequence identity between ApTKI and the templates used for its modeling, an objective validation gives results suggestive of reliable models. ApTKI model construction starts with PSI-BLAST analysis, which was used to select best template. ApTKI sequence was directly compared to amino acid residue sequences that possess structures experimentally resolved and deposited in the Protein Data Bank (PDB) [37]. SKTI presented 37% of identity with ApTKI, being chosen as template. Alignments among sequences and structures were carried by using Clustal-W [38] in order to analyze the primary sequence inhibitor (Fig. 3). The bifunctional inhibitor presented 65% of similarity to the primary sequence of soybean inhibitor for α and β chain. However, comparisons to the Kunitz-type inhibitor from *P. juliflora* presented 67% of identity, the variable being lack of amino acid residues (Trp^{60}, Glu^{89}, and Glu^{109}) involved in *in silico* interaction of PjTKI and papain. The lack of Trp^{60} and Glu^{89} residue substitution for Asp^{89} in ApTKI explains the absence of a loop with appropriate length. This reduction could be related to low affinity for papain and also for a non-competitive mechanism. However the multiple alignments with 1avw demonstrate that the bifunctional inhibitor presents high similarity when secondary structure was compared and the B chain showed 50% of identity with the template.

Table 1
Inhibition assays of ApTKI against trypsin and papain; assays were conducted by using single and also pre-complexed inhibitors against serine- and cysteine-proteinases. Assays were conducted in triplicate (reported ±SD) by using azocasein 1% as substrate.

Treatment	Proteolytic activity (U)	Inhibition (%)
Trypsin	317 ± 12	
Trypsin + ApTKI	10 ± 3	97.0
(Papain + ApTKI) + trypsin	25 ± 4	91.0
Papain	454 ± 10	
Papain + ApTKI	236 ± 10	48.0
(Trypsin + ApTKI) + papain	246 ± 17	46.0

After alignment analysis, atomic coordinates were transferred to ApTKI primary structure. The constructed model displays internal three-fold symmetry, as previously observed in SKTI, and two polypeptide chains linked by a disulfide bridge are similar to Kunitz-type inhibitors from the Mimosoideae family (Fig. 4A). The amino acids were structurally organized in loops connecting consecutive β-strands, a pattern observed in Kunitz inhibitors. Overlap of these domains showed a high similarity among β-strands but not among the connecting loops presenting the classic barrel-shaped structure (Fig. 4B).

Procheck summary of ApTKI showed that 97.9% amino acid residues were in the most favorable region and only three residues (Ser^{37}, Glu^{110} and Asp^{162}) were in the disallowed regions. These residues were presented within loops and as such were

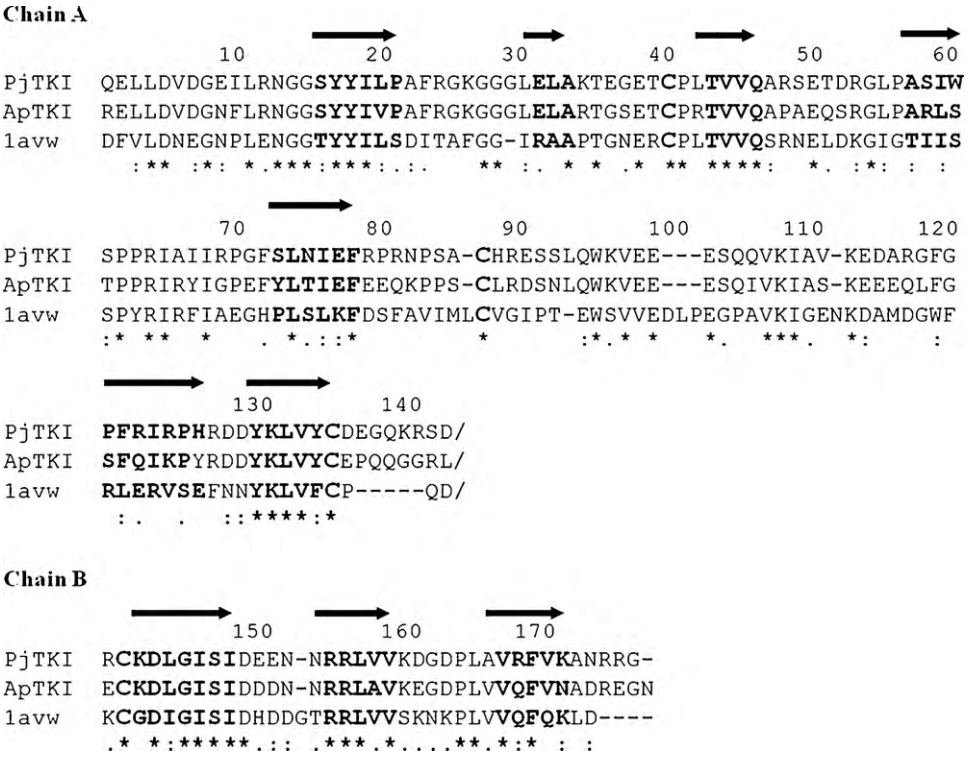

Fig. 3. Multiple sequence alignment of Kunitz bifunctional inhibitors (PjTKI and ApTKI) and template (1avw). Conserved cysteine residues are shown in bold and arrows represent β-sheet in ApTKI. Asterisks indicate conserved residues.

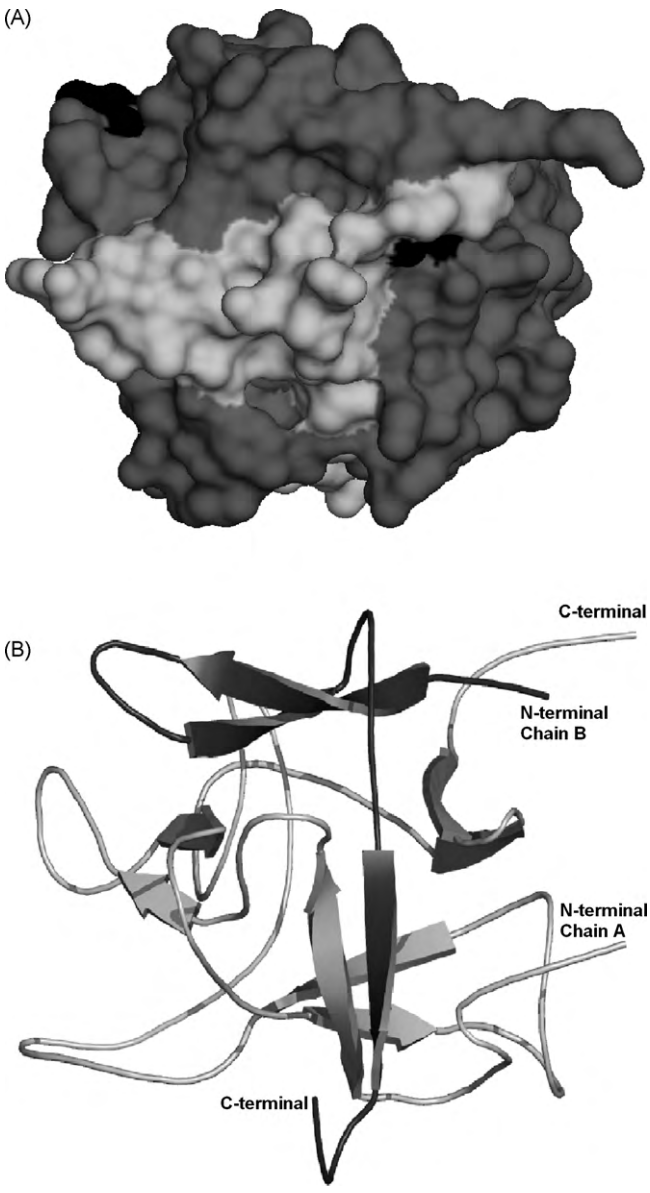

Fig. 4. (A) Surface tridimensional structure of ApTKI demonstrating disulfide bonds in black (B). ApTKI structural model in barrel shape represented in cartoon indicating α (138 amino acid residues) and β chains (38 amino acid residues).

not expected to affect the ApTKI predicted structure. Structural differences between crystal structure of SKTI and predicted three-dimensional structure of the ApTKI model were calculated by superimposing both structures. The RMSD values between the crystal structure of SKTI and homology model of ApTKI calculated for Cα traces and main chain atom were 0.78 Å. The rmsd values and small variability among experimental structures template and the structure modeled reflect the presence of strong restraints in most regions and emphasize a similar folding pattern among these inhibitors. Furthermore, the lower score acquired for PROSA II and high score acquired for overall steric g-factor in the case of the ApTKI were of −5.4 and −0.41, respectively, indicating the high quality of the model. The result indicated that the constructed ApTKI model presented its amino acid residues within the average of the observed parameters. On the other hand, the structure of lateral chains was considered well located, when compared to the experimental structures with the same resolution.

3.4. In silico docking of ApTKI–trypsin

The complex between ApTKI and trypsin structure PDB: 1fn6 [36] was used for the study of the enzyme–inhibitor interaction (Fig. 5A). The model of interaction showed a mechanism of inhibition of the non-competitive type identical *in vitro* to that observed by Prabhu and Pattabiraman [1]. The inhibitor reactive site is able to block substrate access due to five interactions with a most favorable enzyme region, forming a complex with trypsin with a surface area of 1.228 $Å^2$. Those contacts prevent substrate access to enzyme, although no direct reaction with the catalytic site was observed. The NH^+ atom positive charge of Arg^{64} residue in the inhibitor interacted with the OH^- atoms of Ile^{88} and Thr^{90} residue, forming a hydrogen bond of 2.83 and 2.76 Å. A hydrogen bond of 2.94 Å between Arg^{88} and Tyr^{151} was also detected. The hydroxyl from Ser^{107} acts as a proton receptor, while Asn^{143} acts as a related donor. Furthermore, a similar interaction was observed with the amine (donor) from the cationic side chain from Lys^{108} of the inhibitor and hydroxyl from the enzyme side chain of Gly^{219} (residue receptor). In both cases a hydrogen bond was observed (Fig. 5A).

3.5. In silico docking of ApTKI–papain

In the model of the ApTKI inhibitor and the papain PDB: 9pap [35] the inhibitor presented a mechanism of inhibition of the non-competitive type Macedo et al. [7]. This interaction showed lower *in vitro* affinity, which was also observed in *in silico* experiments by few contacts and a low interface surface area of 604 $Å^2$, which is, however, sufficient for cysteine-proteinase inhibition. Proteolytic activity from papain was probably lost due to modifications that occurred in the reactive site, caused by an interaction inhibitor enzyme in the most favorable region. The complex formed between ApTKI and papain is stabilized by three hydrogen bonds formed between Gln^{51} and Gly^{135} residues, with distances of approximately 2.2 Å. An outer hydrogen bond was observed between Arg^{53} and OH^- lateral side in residue Thr^{193}, which acts as a receptor when it finds the proton donor. Finally, a hydrogen bond was formed between the positive-charge Lys^{82} residue and OH^- lateral side in residue Gln^{194}, which reacts with receptor protons (Fig. 5B). In summary, Table 2 shows overall interactions.

It was interesting to note that the *A. pavonina* inhibitor formed a ternary complex with the trypsin and papain, which was demonstrated *in vitro* and confirmed *in silico*. This inhibitor formed a ternary complex through non-competitive mechanisms and was able to prevent the trypsin from interacting strongly with α chain polypeptide and moderately with papain, through β chain polypeptide, indicating that ApTKI is in fact a bifunctional inhibitor, able to act toward two different enzyme classes (Fig. 6).

4. Discussion

Proteinaceous inhibitors have been purified and characterized from a wide variety of plant seeds [5,9,39,40]. The role of these inhibitors as defensive compounds against predators was studied as early as 1947, when Mickel and Standish [41] observed that larvae of certain insects were unable to develop on soybean products. These protein-like inhibitors show molecular masses (20–24 kDa) and primary structures similar to those of α-chain of soybean Kunitz trypsin inhibitor family [42,43] and are reunited in a Kunitz-type proteinase inhibitor superfamily. These include regulation of endogenous enzymes and play a significant role in the defense mechanism of plants against insect and phytopathogen attacks [44–48]. Furthermore, bifunctional inhibitors have been commonly investigated, since these inhibitors are excellent candidates in the transgenic processes and also in the studies of enzyme and inhibitor

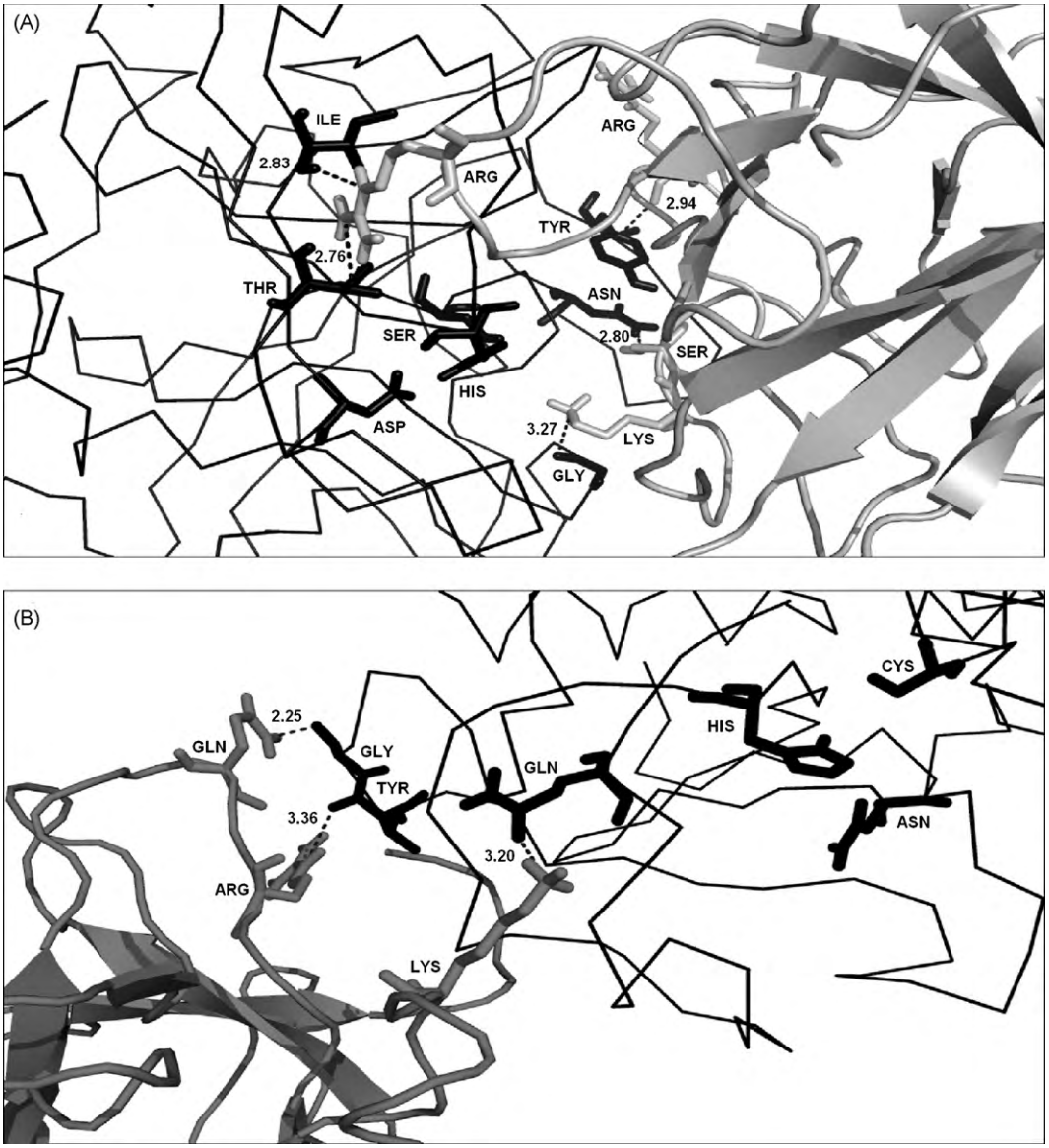

Fig. 5. ApTKI complexed to trypsin (A) and papain (B). The inhibitor backbone is shown as cartoon and proteinase backbone is shown as Cα-traces. Side chain sticks indicate residues involved in enzyme–inhibitor interaction.

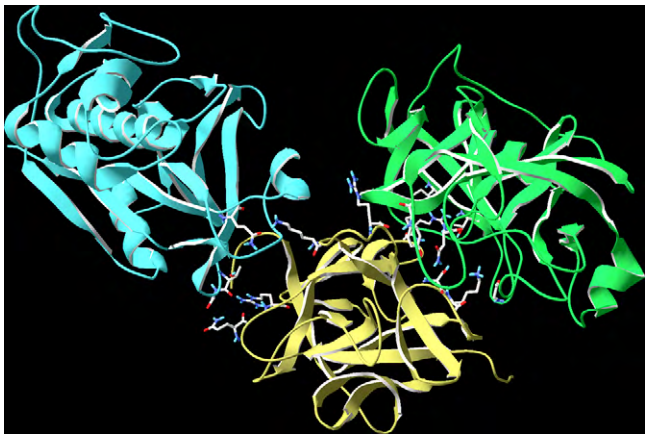

Fig. 6. Visualization of the ternary complex formed in Trypsin (blue)–ApTKI (yellow)–papain (green). Side chain sticks indicate residues involved in enzyme–inhibitor interaction.

specificities [49,50]. Among them, PjTKI, a Kunitz inhibitor from *P. juliflora* seeds, was reported as a rare bifunctional inhibitor with the ability to inhibit two different enzyme classes (serine- and cysteine-proteinases) [6,17]. Recently, ApTKI, a Kunitz inhibitor from *A. pavonina* seeds, which has 88% of similarity with PjTKI, showed similar properties in *in vitro* studies [7]. For this reason this study reports the construction of a three-dimensional model of ApTKI and further *in vitro* and *in silico* evaluations of the inhibitor against the two proteolytical enzymes (trypsin and papain). The ApTKI model showed 38% of identity with Kunitz inhibitor from *Glycine max,* and this identity was observed in other inhibitors utilized for comparative modeling [11,17]. The three-dimensional inhibitor model present two polypeptide chains with twelve antiparallel β-sheets connected for long loops forming a beta barrel. This structural fold is commonly found in beta family Kunitz-type inhibitors resolved by X-ray diffraction, such as *G. max*, *D. regia*, *E. caffra*, *C. langsdorffii* and *P. tetragonolobus* [13–15,51,52]. The two polypeptide chains (one major, one minor) linked by disulfide bonds, found in ApTKI, are also observed in other Kunitz-type trypsin inhibitors found in the Mimosoideae subfamily, such as seeds of *A. ellipticum* [2], *L. leu-*

cocephala [11], *E. contortisiliquum* [20], *A. elata* [53], *A. confusa* [54] and *P. dulce* [55]. Otherwise, some Kunitz-type inhibitors, such as *P. dumosum* [22], *E. scandens* [56] and *I. laurina* seeds [57], are examples of a single polypeptide chain from Mimosoideae subfamily, confirming the varied nature of this subclass of protease inhibitors.

The validation of the 3D model of ApTKI by PROSA II program and Ramachandran plot showed that the model presented 97.9% of the amino acid residues in physically acceptable regions, with 88.9% of the situated residues in more favorable regions, 9.0% occurring in allowed regions, 0.7% are in generously allowed regions and three residues Ser^{37}, Glu^{110} and Asp^{162} only in disallowed regions for secondary structure formation in relation to torsion angles phi and psi. This result is in agreement with those found for the *L. leucocephala* Kunitz-type inhibitor [11], which was constructed by comparative modeling. The structural overlapping between ApTKI and SKTI (pdb: 1avw) presented a value of RMSD 0.78 Å, more that observed for the model of *L. leucocephala* inhibitor that presented values of RMSD for crystals of SKTI:PPT (ortho and tetragonal) between 0.58 and 0.47 Å. The Ramachandran plot and the value of RMSD of ApTKI demonstrated that the inhibitor model is acceptable [11]. In addition, the value of PROSA II was of −5.4, similar to that found in the model constructed with the same template of *P. juliflora,* which presented −5.0 for the models constructed with the template, placing 90–91% of residues in physically favorable regions of the Ramachandran plot [17].

Protein–protein interface server analysis (PPIS) of the most favored ApTKI–trypsin and template reveals several properties involving the relation of interface and surface area. The SKTI–trypsin complex presented 803 $Å^2$ compared to 1.228 $Å^2$ in the ApTKI–trypsin. Other PPIS parameters are nearly identical, with a single exception. The minor gap volume index of the model (3.04 compared to 3.41 of the template) highlights significantly higher complementarity. Having established the benchmark for acceptable quality of the ApTKI model, the best PROSA II scores were used in docking experiments with the HEX v5.1 suite of programs [58,59]. The top 50 docking solutions of 500 interaction results were screened for the model with the PPIS. The top-ranking HEX v5.1 result was also clearly favored by PPIS analysis, having an interface surface area of 1228 $Å^2$ and a gap volume index of 3.04. These data compare well with values for all known enzyme–inhibitor complexes of 785 $Å^2 \pm 75$ (mean ± SD) and 2.2 ± 0.5, respectively, a surprising complementarity [60].

The 3D models of interaction of ApTKI with trypsin showed an inhibition mechanism of non-competitive type, in agreement with data presented by Prabhu and Pattabiraman [1] and Macedo et al. [7]. Hydrogen bonds in the ApTKI-trypsin interaction presented five polar contacts, with distances of 2.83 and 2.76 Å between Arg^{64} of the inhibitor and Ile^{88} and Thr^{90} of the enzyme. Moreover, Ser^{107} from inhibitor showed a hydrogen bond with Asn^{143} of enzyme, at a distance of 2.80 Å. Lys^{108} residue forms a hydrogen bond with Asn^{143} with distance 3.27 Å. Outer polar interaction was observed between Arg^{88} and Tyr^{151} with distance of 2.95 Å. These distances were similar to those found for the LTI:PPT complex of *L. leucocephala* inhibitor with trypsin, which showed distances between the Arg^{62} and the Ser^{195} of 2.76 Å and 2.71 Å, for the models constructed by using crystallized soybean inhibitor as template [11,13]. This non-competitive inhibition type observed in ApTKI presented a complementary superficial area higher than that observed in PjTKI, which shows remarkable affinity [17]. The Asn^{13} residue in ApTKI model interacts by a hydrogen bond with amino acid residue Arg^{64}. In the tertiary structure, the formation of the polar contact with the residue Arg^{64} leads to a loop stabilization. Iwanaga et al. [21] reported that Kunitz-type inhibitors have usual structural properties where Asn^{13} residue is conserved and play a role in the inhibitory activity, since this residue forms an intra-chain hydrogen bond with reactive loop residues. The alignment between ApTKI and 1avw showed that Asn^{13} is extremely well conserved. Another similar result was observed for the *P. tetragonolobus* Kunitz inhibitor, which presented the Asn^{14} residue with an important role in the stability and conformation of its reactive loop [61].

The ApTKI–papain complex presents structural differences, especially in the interface area, when compared to the PjTKI–papain model. These substitutions lead to gaps at the interface, reducing complementarity. Some of these modifications might lead to the ordering of water molecules, an entropically unfavorable process, and hence contribute to a lesser ApTKI affinity for papain compared to the PjTKI model [17]. The most favored HEX v5.1 result presented an interface surface area of 604 $Å^2$ and a complementarity gap volume index score of 3.3. Planarity and circularity values [60] of 2.14 and 0.77 are also typical. No other solutions had favorable combinations of large interface area and good complementarity; the mean values among the 50 analysis solutions were 454 ± 71 $Å^2$ and 5.4 ± 1.0 (mean ± SD). The values were also similar where compared with interface area and complementarity in enzyme–inhibitor complexes with their upper limits at 785 $Å^2 \pm 75$ and 2.2 ± 0.5, respectively. Planarity and circularity values of 2.14 and 0.77, where compared with PjTKI, confirmed papain's low affinity, as showed *in vitro* [17]. The lack of overlap among ApTKI tryptophan residues predicted to bind to trypsin and papain is showed outside the loop for papain observed in PjTKI (Fig. 5). Examination of the HMM-constructed alignment of all 143 homologs in the nr database reveals that a tryptophan is only present in this position in one other protein: the *A. confusa* trypsin inhibitor (ITRY_ACACO)[54] indicating that this residue plays an important role in competitive interaction. Hydrophobic and electrostatic considerations are among the most important aspects of protein–protein interfaces, as reflected in the special attention afforded to them by docking programs [58,62]. The scarcity of residues corresponding to PjTKI (Trp^{60}, Glu^{89}, and Glu^{109}) in other Kunitz homologs may therefore explain the rarity of papain competitive inhibition within the family. On the other hand, the occurrence of non-competitive inhibition presented in ApTKI may be visualized in the positive-charged region.

The 3D models of interaction of ApTKI with papain also showed an inhibition mechanism of non-competitive type, in agreement with the results of Macedo et al. [7], and the interaction sites to trypsin and papain did not overlap with those seen in PjTKI. This result was different to those found for PjTKI, which presented reactive sites overlapped with papain and trypsin [17]. In comparison with PjTKI, the inhibition of papain by ApTKI was lower; this fact could be explained by changes in the residues of the inhibitor that were involved in the interaction with the papain observed in alignment. These changes were noted when the primary sequence was analyzed and further compared. Interaction site of PjTKI–papain (Trp^{60}, Arg^{64}, Glu^{89} and Glu^{109}) and complex ApTKI-papain (Asp^{140}, Lys^{190} and Thr^{193}) were compared in multiple alignments (Fig. 3) showing that amino acid residue Glu^{109} was conserved and Glu^{89}

Table 2
ApTKI interactions with trypsin and papain. Contacts in binding sites were proposed by protein–protein interaction server. HB corresponds to hydrogen bond.

Protein residues	Protein residues	Interaction
Trypsin	*Inhibitor*	
Ile^{88}	Arg^{64}	HB
Thr^{90}	Arg^{64}	HB
Asn^{143}	Ser^{107}	HB
Tyr^{151}	Arg^{88}	HB
Gly^{219}	Lys^{108}	HB
Papain	*Inhibitor*	
Gly^{135}	Gln^{51}	HB
Thr^{193}	Arg^{53}	HB
Gln^{194}	Lys^{82}	HB

was replaced by Asp^{89}, a shorter amino acid with similar properties. Also, the absence of Trp^{60} could explain the moderate efficiency of the inhibition of ApTKI to papain and the overlapping demonstrated in PjTKI [17]. The Trp^{60} in PjTKI–papain complex was responsible for high specificity to papain, since side chains of aromatic (Trp^{69}, Tyr^{67}) and cationic (Arg^{59}) residues from papain are able to interact with the inhibitor by van der Waals forces. Another indication that suggests lower affinity of inhibitor ApTKI was the reduced complementary superficial area observed. In the inhibitor ApTKI an area of 604 $Å^2$ was seen, which is half of that demonstrated in PjTKI, which presented 1387 $Å^2$. This fact reflects why *in vitro* assays demonstrated that ApTKI showed 50% of inhibition when compared to experimental data developed with PjTKI [17]. In addition, the occurrence of switching reactive site loops for double-headed inhibitors is not unique to ApTKI and PjKTI, also having been proposed for winged bean chymotrypsin inhibitor crystal structure and recently for *S. sagittifolia* outer Kunitz inhibitor with resolution 2.48 Å [52,63]. The reactive sites of all these inhibitors could have evolved from variable loops of ancestral Kunitz-type proteins that generate numerous inhibitory possibilities, improving specificities and diverging from the action mechanism of plant defense proteins studied here [17,52,63].

5. Conclusion

In summary, a purified inhibitor from *A. pavonina* seeds presented trustworthy 3D structure, after several validations. The *in vitro* and *in silico* studies demonstrated that ApTKI was a strong non-competitive inhibitor of trypsin and moderate non-competitive inhibitor to papain. The interaction sites of the ApTKI did not overlap, and it formed a ternary complex that was observed through *in vitro* and *in silico* methods. This inhibitor had an interesting and exclusive ability to interact with two different proteinase classes, serine (trypsin) and cysteine (papain); it is thus able to contribute to development of biotechnological tools such as transgenic plants with enhanced resistance to insect-pests. Moreover, data reported here gives novel insights into non-competitive mechanisms of the Kunitz inhibitors, providing some target residues that could be utilized in the near future to construct mutants and further validating information obtained here.

Acknowledgments

This study was supported by the following Brazilian Agencies: FINEP, CAPES, FAPDF, FAPEMIG, CNPq, and BNB-FUNDECI.

References

[1] K.S. Prabhu, T.N. Pattabiraman, Natural plant enzyme–inhibitors—isolation and characterization of a trypsin–chymotrypsin inhibitor from Indian Red Wood (*Adenanthera pavonia*) seeds, Journal of the Science of Food and Agriculture 31 (1980) 967–980.
[2] A. Bhattacharyya, S. Mazumdar, S.M. Leighton, C.R. Babu, A Kunitz proteinase inhibitor from *Archidendron ellipticum* seeds: purification, characterization, and kinetic properties, Phytochemistry 67 (2006) 232–241.
[3] A.S. Oliveira, L. Migliolo, R.O. Aquino, J.K.C. Ribeiro, L.L.P. Macedo, L.B.S. Andrade, M.P. Bemquerer, E.A. Santos, S. Kiyota, M.P. Sales, Identification of a Kunitz-type proteinase inhibitor from *Pithecellobium dumosum* seeds with insecticidal properties and double activity, Journal of Agricultural and Food Chemistry 55 (2007) 7342–7349.
[4] M.L.R. Macedo, D.G.G. Matos, O.L.T. Machado, S. Marangoni, J.C. Novello, Trypsin inhibitor from *Dimorphandra mollis* seeds: purification and properties, Phytochemistry 54 (2000) 553–558.
[5] G.C. Mello, M.L.V. Oliva, J.T. Sumikawa, O.L.T. Machado, S. Marangoni, J.C. Novello, M.L. Macedo, Purification and characterization of a new trypsin inhibitor from *Dimorphandra mollis* seeds, Journal of Protein Chemistry 20 (2001) 625–632.
[6] A.S. Oliveira, R.A. Pereira, L.M. Lima, A.H.A. Morais, F.R. Melo, O.L. Franco, C. Bloch Jr., M.F. Grossi-de-Sá, M.P. Sales, Activity toward bruchid pest of a Kunitz-type inhibitor from seeds of the algaroba tree (*Prosopis juliflora* DC), Pesticide Biochemistry and Physiology 72 (2002) 122–132.
[7] M.L.R. Macedo, C.M. De Sa, M.D.M. Freire, J.R.P. Parra, A Kunitz-type inhibitor of coleopteran proteases, isolated from *Adenanthera pavonina* L. seeds and its effect on *Callosobruchus maculatus*, Journal of Agricultural and Food Chemistry 52 (2004) 2533–2540.
[8] V.D.S. Ramos, G.N.D.S. Silva, M.D.G.A.M. Freire, O.L.T. Machado, J.R.P. Parra, M.L.G.R. Macedo, Purification and characterization of a trypsin inhibitor from *Plathymenia foliolosa* seeds, Journal of Agricultural and Food Chemistry 56 (2008) 11348–11355.
[9] A.N. Negreiros, M.M. Carvalho, J. Xavier Filho, A. Blanco-Labra, P.R. Shewry, M. Richardson, The complete amino acid sequence of the major Kunitz trypsin inhibitor from the seeds of *Prosopsis juliflora*, Phytochemistry 30 (1991) 2829–2833.
[10] H.C. Wu, J.Y. Lin, The complete amino acid sequence of a Kunitz family trypsin inhibitor from seeds of *Acacia confusa*, Journal of Biochemistry 113 (1993) 258–263.
[11] R. Sattar, S.A. Ali, M. Kamal, A.A. Khan, A. Abbasi, Molecular mechanism of enzyme inhibition: prediction of the three-dimensional structure of the dimeric trypsin inhibitor from *Leucaena leucocephala* by homology modelling, Biochemical and Biophysical Research Communications 314 (2004) 755–765.
[12] J. Xavier-Filho, The biological roles of serine and cysteine proteinase inhibitors in plants, Revista Brasileira de Fisiologia 4 (1992) 1–6.
[13] H.K. Song, S.W. Suh, Kunitz-type soybean trypsin inhibitor revisited: refined structure of its complex with porcine trypsin reveals an insight into the interaction between a homologous inhibitor from *Erythrina caffra* and tissue-type plasminogen activator, Journal of Molecular Biology 275 (1998) 347–363.
[14] S. Krauchenco, R.A.P. Nagem, J.A. da Silva, S. Marangoni, I. Polikarpov, Three-dimensional structure of an unusual Kunitz (STI) type trypsin inhibitor from *Copaifera langsdorffii*, Biochimie 86 (2004) 167–172.
[15] S. Krauchenco, S.C. Pando, S. Marangoni, I. Polikarpov, Crystal structure of the Kunitz (STI)-type inhibitor from *Delonix regia* seeds, Biochemical and Biophysical Research Communications 312 (2003) 1303–1308.
[16] S. Khamrui, H. Dasgupta, J.K. Dattagupta, U. Sen, Single mutation at P1 of a chymotrypsin inhibitor changes it to a trypsin inhibitor: X-ray structural (2.15 angstrom) and biochemical basis, Biochimica et Biophysica Acta Proteins & Proteomics 1752 (2005) 65–72.
[17] O.L. Franco, M.F. Grossi de Sá, M.P. Sales, L.V. Mello, A.S. Oliveira, D.J. Rigden, Overlapping binding sites for trypsin and papain on a Kunitz-type proteinase inhibitor from *Prosopis juliflora*, Proteins 49 (2002) 335–341.
[18] A. Bhattacharyya, S.M. Leighton, C.R. Babu, Bioinsecticidal activity of *Archidendron ellipticum* trypsin inhibitor on growth and serine digestive enzymes during larval development of *Spodoptera litura*, Comparative Biochemistry and Physiology C-Toxicology & Pharmacology 145 (2007) 669–677.
[19] C.H. Hung, M.C. Lee, J.Y. Lin, Inactivation of *Acacia confusa* trypsin–inhibitor by site-specific mutagenesis, FEBS Letters 353 (1994) 312–314.
[20] I.F.C. Batista, M.L.V. Oliva, M.S. Araujo, M.U. Sampaio, M. Richardson, H. Fritz, C.A.M. Sampaio, Primary structure of a Kunitz-type trypsin inhibitor from *Enterolobium contortisiliquum* seeds, Phytochemistry 41 (1996) 1017–1022.
[21] S. Iwanaga, N. Yamasaki, M. Kimura, Y. Kouzuma, Contribution of conserved Asn residues to the inhibitory activities of Kunitz-type protease inhibitors from plants, Bioscience Biotechnology and Biochemistry 69 (2005) 220–223.
[22] M.S.M. Cavalcanti, M.L.V. Oliva, H. Fritz, M. Jochum, R. Mentele, M. Sampaio, L.C.B.B. Coelho, I.F.C. Batista, C.A.M. Sampaio, Characterization of a Kunitz trypsin inhibitor with one disulfide bridge purified from *Swartzia pickellii*, Biochemical and Biophysical Research Communication 291 (2002) 635–639.
[23] C.E. Gomes, A.E. Barbosa, L.L. Macedo, J.C. Pitanga, F.T. Moura, A.S. Oliveira, R.M. Moura, A.F.S. Queiroz, F.P. Macedo, L.B.S. Andrade, M.S. Vidal, M.P. Sales, Effect of trypsin inhibitor from *Crotalaria pallida* seeds on *Callosobruchus maculatus* (cowpea weevil) and *Ceratitis capitata* (fruit fly), Plant Physiology Biochemical 43 (2005) 1095–1102.
[24] S.C. Pando, M.L.V. Oliva, C.A.M. Sampaio, L. Di Ciero, J.C. Novello, S. Marangoni, Primary sequence determination of a Kunitz inhibitor isolated from *Delonix regia* seeds, Phytochemistry 57 (2001) 625–631.
[25] J. Langner, A. Wakil, M. Zimmermann, S. Ansorge, P. Bohley, H. Kirschke, Activity determination of proteolytic enzymes using azocasein as a substrate, Acta Biologica et Medica Germanica 31 (1973) 1–18.
[26] M. Richardson, F.A.P. Campos, J. Xavier-Filho, M.L.R. Macedo, G.M.C. Maia, A. Yarwood, The amino-acid-sequence and reactive (inhibitory) site of the major trypsin isoinhibitor (De5) isolated from seeds of the Brazilian Carolina tree (*Adenanthera pavonina* L.), Biochimica et Biophysica Acta 872 (1986) 134–140.
[27] S.F. Altschul, W. Gish, W. Miller, E.W. Myers, D.J. Lipman, Basic Local Alignment Search Tool, Journal of Molecular Biology 215 (1990) 403–410.
[28] N. Eswar, B. Webb, M.A. Marti-Renom, M.S. Madhusudhan, D. Eramian, M.Y. Shen, U. Pieper, A. Sali, Comparative protein structure modeling using MODELLER, Current Protocols in Protein Science (2007) (Chapter 2, Unit 29).
[29] K. Arnold, L. Bordoli, J. Kopp, T. Schwede, The SWISS-MODEL workspace: a web-based environment for protein structure homology modelling, Bioinformatics (Oxford, England) 22 (2006) 195–201.
[30] M. Wiederstein, M.J. Sippl, ProSA-web: interactive web service for the recognition of errors in three-dimensional structures of proteins, Nucleic Acids Research 35 (2007) W407–W410.
[31] R.A. Laskowski, M.W. Macarthur, D.S. Moss, J.M. Thornton, Procheck—a program to check the stereochemical quality of protein structures, Journal of Applied Crystallography 26 (1993) 283–291.
[32] K. Sumathi, P. Ananthalakshmi, M.N. Roshan, K. Sekar, 3dSS: 3D structural superposition, Nucleic Acids Research 34 (2006) W128–W132.

[33] N. Guex, M.C. Peitsch, SWISS-MODEL and the Swiss-PdbViewer: an environment for comparative protein modeling, Electrophoresis 18 (1997) 2714–2723.
[34] D.W. Ritchie, Recent progress and future directions in protein–protein docking, Current Protein & Peptide Science 9 (2008) 1–15.
[35] I.G. Kamphuis, K.H. Kalk, M.B. Swarte, J. Drenth, Structure of papain refined at 1.65 Å resolution, Journal Molecular Biology 179 (1984) 233–256.
[36] S. Deepthi, A. Johnson, V. Pattabhi, Structures of porcine beta-trypsin–detergent complexes: the stabilization of proteins through hydrophilic binding of polydocanol, Acta Crystallography 57 (2001) 1506–1512.
[37] H.M. Berman, J. Westbrook, Z. Feng, G. Gilliland, T.N. Bhat, H. Weissig, I.N. Shindyalov, P.E. Bourne, The Protein Data Bank, Nucleic Acids Research 28 (2000) 235–242.
[38] J.D. Thompson, D.G. Higgins, T.J. Gibson, Clustal-W—Improving the sensitivity of progressive multiple sequence alignment through sequence weighting, position-specific gap penalties and weight matrix choice, Nucleic Acids Research 22 (1994) 4673–4680.
[39] M.L.R. Macedo, J. Xavier Filho, Purification and partial characterization of trypsin–inhibitors from seeds of *Clitoria ternatea*, Journal of the Science of Food and Agriculture 58 (1992) 55–58.
[40] C.L. Araujo, I.W.L. Bezerra, A.S. Oliveira, F.T. Moura, L.L.P. Macedo, C.E.M. Gomes, *In vivo* bioinsecticidal activity toward *Ceratitis capitata* (Fruit fly) and *Callosobruchus maculatus* (Cowpea weevil) and *in vitro* bioinsecticidal activity toward different orders of insect pests of a trypsin inhibitor purified from tamarind tree (*Tamarindus indica*) seeds, Journal of Agricultural and Food Chemistry 53 (2005) 4381–4387.
[41] C.E. Mickel, J. Standish, Susceptibility of processed soy flour and soy grits in storage to attack by *Tribolium castaneum*, in: University of Minnesota Agricultural Experimental Station Technical Bulletin, University of Minnesota, St. Paul, MN, 1947, pp. 1–20.
[42] A.M.R. Gatehouse, D. Boulter, Assessment of the antimetabolic effects of trypsin inhibitors on the development of the bruchid beetle, *Callosobruchus maculatus*, Journal of the Science of Food and Agriculture (1983) 345–350.
[43] I. Krizaj, M. Drobnic-Kosorok, J. Brzin, R. Jerala, V. Turk, The primary structure of inhibitor of cysteine proteinases from potato, FEBS Letters 333 (1993) 15–20.
[44] T.A. Walsh, W.P. Twitchell, Two Kunitz-type proteinase inhibitors from potato tubers, Plant Physiology 97 (1991) 15–18.
[45] A. Ishikawa, S. Ohta, K. Matsuoka, T. Hattori, K. Nakamura, A family of potato genes that encode Kunitz-type proteinase inhibitors: structural comparisons and differential expression, Plant & Cell Physiology 35 (1994) 303–312.
[46] M. Richardson, Seed storage proteins: the enzyme inhibitors, Methods in Plant Biochemistry 5 (1991) 259–305.
[47] P.K. Lawrence, K.R. Koundal, Plant protease inhibitors in control of phytophagous insects, Electronic Journal of Biotechnology 5 (2002).
[48] P.R. Shewry, J.A. Lucas, Plant proteins that confer resistance to pests and pathogens, Advances in Botanical Research Incorporating Advances in Plant Pathology 26 (1997) 135–192.
[49] K.J. Zenke, A. Muller-Fahrnow, M.D. Jany, G.P. Pal, W. Saenger, The three-dimensional structure of the bifunctional proteinase K/α-amylase inhibitor from wheat (PKI3) a 2.5 Å resolution, FEBS Letters 279 (1991) 240–242.
[50] A. Furtado, R. Henry, K. Scott, S. Meech, The promoter of the asi gene directs expression in the maternal tissues of the seed in transgenic barley, Plant Molecular Biology 52 (2003) 787–799.
[51] S. Onesti, P. Brick, D.M. Blow, Crystal structure of a Kunitz-type trypsin inhibitor from *Erythrina caffra* seeds, Journal Molecular Biology 217 (1991) 153–176.
[52] J.K. Dattagupta, A. Podder, C. Chakrabarti, U. Sen, D. Mukhopadhyay, S.K. Dutta, M. Singh, Refined crystal structure (2.3 Å) of a double-headed winged bean alpha-chymotrypsin inhibitor and location of its second reactive site, Proteins 35 (1999) 321–331.
[53] A.A. Kortt, M.A. Jermyn, *Acacia* proteinase-inhibitors—purification and properties of the trypsin–inhibitors from *Acacia elata* seed, European Journal of Biochemistry 115 (1981) 551–557.
[54] J.Y. Lin, S.C. Chu, H.C. Wu, Y.S. Hsieh, Trypsin–inhibitor from the seeds of *Acacia confusa*, Journal of Biochemistry 110 (1991) 879–883.
[55] F.D. Vargas, H.E.L. Valdes, S.V. Rodriguez, A.B. Labra, A.C. Lopez, E.J.L. Valenzuela, Isolation and properties of a Kunitz-type protein inhibitor obtained from *Pithecellobium dulce* seeds, Journal of Agricultural and Food Chemistry 52 (2004) 6115–6121.
[56] M.H. Lingaraju, L.R. Gowda, A Kunitz trypsin inhibitor of *Entada scandens* seeds: another member with single disulfide bridge, Biochimica et Biophysica Acta 1784 (2008) 850–855.
[57] M.L.R. Macedo, V.A. Garcia, M.D.M. Freire, M. Richardson, Characterization of a Kunitz trypsin inhibitor with a single disulfide bridge from seeds of *Inga laurina* (SW.) Willd., Phytochemistry 68 (2007) 1104–1111.
[58] H.A. Gabb, R.M. Jackson, M.J. Sternberg, Modelling protein docking using shape complementarity, electrostatics and biochemical information, Journal Molecular Biology 272 (1997) 106–120.
[59] G. Moont, H.A. Gabb, M.J. Sternberg, Use of pair potentials across protein interfaces in screening predicted docked complexes, Proteins 35 (1999) 364–373.
[60] S. Jones, J.M. Thornton, Principles of protein–protein interactions, Proceedings of the National Academy of Sciences of the United States of America 93 (1996) 13–20.
[61] S. Ravichandran, J. Dasgupta, C. Chakrabarti, S. Ghosh, M. Singh, J.K. Dattagupta, The role of Asn14 in the stability and conformation of the reactive-site loop of winged bean chymotrypsin inhibitor: crystal structures of two point mutants asn14 → Lys and Asn14 → Asp, Protein Engineering 14 (2001) 349–357.
[62] I.A. Vakser, C. Aflalo, Hydrophobic docking: a proposed enhancement to molecular recognition techniques, Proteins 20 (1994) 320–329.
[63] R. Bao, C.Z. Zhou, C. Jiang, S.X. Lin, C.W. Chi, Y. Chen, The ternary structure of the double-headed arrowhead protease inhibitor API-A complexed with two trypsins reveals a novel reactive site conformation, Journal of Biological Chemistry 28 (2009) 1–21.